Molecular Vision 2007; 13:1746-57 <http://www.molvis.org/molvis/v13/a195/>
Received 12 June 2007 | Accepted 14 August 2007 | Published 19 September 2007

Glucocorticoids induce retinal toxicity through mechanisms mainly associated with paraptosis

Fatemeh Valamanesh,[1,2] Alicia Torriglia,[1] Michéle Savoldelli,[1,3] Christelle Gandolphe,[1] Jean-Claude Jeanny,[1] David BenEzra,[1,4] Francine Behar-Cohen[1,2,3]

[1]INSERM, Physiopathology of ocular diseases: Therapeutic innovations, Institut des Cordeliers, 15 Rue de L'Ecole de Médecine, Université René Descartes; [2]Laboratoire d'Innovations Thérapeutiques, Fondation Rothschild; [3]Université René Descartes, Hotel Dieu University hospital, Paris, France; [4]Hadassah Hebrew University Hospital, Jerusalem, Israel

Purpose: Corticosteroids have recorded beneficial clinical effects and are widely used in medicine. In ophthalmology, besides their treatment benefits, side effects, including ocular toxicity have been observed especially when intraocular delivery is used. The mechanism of these toxic events remains, however, poorly understood. In our present study, we investigated the mechanisms and potential pathways of corticosteroid-induced retinal cell death.
Methods: Rats were sacrificed 24 h and 8 days after an intravitreous injection of 1 µl (40 µg) of Kenacort Retard®. The eyes were processed for ultra structure analysis and detection of activated caspase-3, cytochrome-C, apoptosis-inducing factor (AIF), LEI-L-Dnase II, terminal transferase dUTP nick end labeling (TUNEL), and microtubule-associated protein 1-light chain 3 (MAP-LC3). In vitro, rat retinal pigment epithelial cells (RPE), retinal Müller glial cells (RMG) and human ARPE-19 cells were treated with triamcinolone acetonide (TA) or other glucocorticoids. Cell viability was quantified by 3-(4,5-dimethylthiazol-2-yl)-2,5 phenyltetrazolium bromide test (MTT) assay and cell counts. Nuclei staining, TUNEL assay, annexin-V binding, activated caspase-3 and lactate dehydrogenase (LDH) production characterized cell death. Localization of cytochrome-C, AIF, LEI-and L-Dnase II, and staining with MAP-LC3 or monodansylcadaverine were also carried out. Finally, ARPE-19 cells transfected with AIP-1/Alix were exposed to TA.
Results: In vitro incubation of retinal cell in the presence of corticosteroids induced a specific and dose-dependent reduction of cell viability. These toxic events were not associated with the anti-inflammatory activity of these compounds but depended on the hydro solubility of their formulation. Before cell death, extensive cytoplasmic vacuolization was observed in the retinal pigment epithelial (RPE) cells in vivo and in vitro. The cells however, did not show known caspase-dependent or caspase-independent apoptotic reactions. These intracellular vacuoles were negative for MAP-LC3 but some stained positive for monodansylcadaverine. Furthermore, over expression of AIP-1/Alix inhibited RPE cell death.
Conclusions: These observations suggest that corticosteroid-induced retinal cell death may be carried out mainly through a paraptosis pathway.

Intravitreal triamcinolone acetonide (TA; Kenalog® or Kenacort® Retard, Bristol-Meyers Squibb, Princeton, NJ) is widely used for the treatment of macular oedema [1-4], ocular inflammation [5-7] and ocular neovascularization [8-10]. This specific corticosteroid formulation has been selected for intravitreal injection because of its sustained effect [11]. The observed long lasting effect of TA is due to its very low intraocular solubility. Long term visual acuity improvement is observed in about 50% of patients treated for macular edema after repeated injections [1].

In the rabbit eye, after one single intravitreal injection of TA, no influence on the global ERG responses were detected [12-14]. In vitro, TA induces a clear toxic effect on retinal pigment epithelial cells (RPE), retinal glial Müller cells (RMG) and retinal neurosensory cells [15-17]. It has been reported that the glucocorticoid retinal cells cytotoxicity in vitro is mediated through alterations of mitochondrial activity [15,17]. More recently, it was shown that the crystalline form and the soluble form of TA have different toxic effects while the vehicle (benzyl alcohol), present in the injected preparation, may contribute to enhance the cellular toxicity [18,19]. Because they are widely and increasingly used in various ocular diseases, more efficient and specifically targeted effects of corticosteroids are needed. To achieve these aims, a better understanding and characterization of the glucocorticoids influence on eye tissues is essential. The aim of the present study is to thoroughly analyze the potential deleterious effects of glucocorticoids on ocular cell and tissues.

During pathological processes cell death is essentially carried out either through passive pathways as cell necrosis or through active and programmed cell death [20]. The caspase-dependent apoptosis is the most widely studied and characterized pathway of programmed cell death [21]. More recently, other forms of active cell death are being recognized [22] and their role in tissue homeostasis and pathology unveiled [23]. Autophagic cell death, for instance, is an evolutionary conserved mechanism allowing the cells to eliminate unnecessary organelles and recycle their own proteins. In neural cells, autophagy is essential for cell survival but when over acti-

Correspondence to: Prof. Francine Behar-Cohen, INSERM UMRS 872 eq. 17, Institut des Cordeliers, 15, rue de l'Ecole de Médecine, 75006, Paris, Phone: 33 1 40 46 78 46; FAX: 33 1 40 46 78 55; email: behar@idf.inserm.fr

vated may also lead to cell death [24,25]. Recently, an additional cytoplasmic programmed cell death mechanism coined paraptosis has been described [26-29].

In this study, we have investigated the involvement of various potential cell death mechanisms induced by corticosteroids in vitro and in vivo.

METHODS

Reagents: All culture reagents were obtained from (Gibco, New York, NY). Corticosteroids were purchased from Sigma (Saint-Quentin Fallavier, France) except for Kenacort Retard® purchased from Bristol-Myers Squibb, (Paris, France).

Intravitreous injection of Kenacort retard in rats: The use of animals adhered to the ARVO statement for Ophthalmic and Vision Research and protocols were approved by the ethical committee of René Descartes University of Paris. Twelve Lewis rats (6-8 weeks-old) received 1 µl of Kenacort Retard® (40 mg/ml) in the vitreous of one eye, using disposable micro fine syringes and 30G needle (Beckton Dickinson, Spain) and 1 µl sterile BSS (Alcon, Rueil Malmaison, France) in the other eye. Twenty-four h (n=4) and 8 days after injection (n=8), rats were sacrificed using a lethal dose of pentobarbital. Out of the 8 rats sacrificed at 8 days after injection, the eyes of 4 rats were used for semi-thin and transmission electron microscopy (TEM) analysis and the 4 other rat eyes were used for cryosections.

Structure analysis: After sacrifice, the eyes were enucleated and fixed in 2.5% glutaraldehyde cacodylate buffer (Na 0.1 M, pH 7.4) for 1 h, then dissected and the posterior segments fixed for 3 h. Specimens were fixed in 1% osmium tetroxyde in cacodylate buffer (Na 0.1 M, pH 7.4) and progressively dehydrated in graduated ethanol solution (50, 70, 95, and 100%). Each posterior segment was separated in 2 samples, included in epoxy resin and oriented. Semi-thin sections (1 µm) were obtained with an ultra microtome Reichert Ultracut (Leica, Switzerland) and stained with toluidin blue. Ultra-thin sections (80 nm) were contrasted by uranyl acetate and lead citrate, and analysed with a Philips CM10 electron microscope.

Immunochemical analysis: For immunohistochemistry, rat eyes were fixed in 4% paraformaldehyde (Merck Eurolab, Fontenay Sous-Bois, France) for 2 h, then rinsed with phosphate buffered saline (PBS), and cryo-protected with sucrose 5, 10, and 15% (1 h, 1 h, and overnight, respectively). Eyes were included in optimal cutting temperature (OCT) compound (Tissue-Tek, Sakura, Zoeterwoude, Netherlands), snap frozen and cryo-sectioned (7 µm thick). Sections were fixed in 4% paraformaldehyde, rinsed with PBS and incubated in 0.1% Triton X-100 (Sigma-Aldrich)-PBS for 30 min. Non-specific fixation sites were saturated with 5% skimmed milk in PBS for 1 h, and then incubated 1 h with one of the following antibodies:

Anti-active caspase-3 polyclonal rabbit antibody (BD. Pharmingen, San Diego, CA) diluted (1/50) in PBS containing 1% bovine serum albumin (BSA).

Anti-L-DNase II polyclonal rabbit antibody [30,31] was diluted (1/100) in PBS containing 1% skimmed milk.

Anti-MAP LC3 polyclonal goat antibody (Santa Cruz biotechnology, Heidelberg, Germany) was diluted (1/50) in PBS containing 1% BSA [32,33].

After incubation with the specific primary antibodies, the sections were rinsed (3 times 5 min each) with PBS, incubated for 1 h at room temperature with rabbit anti-goat IgG (Jackson Immuno Research laboratories INC, Suffolk, UK) washed and incubated with goat anti-rabbit IgG (Molecular Probes) diluted (1/250) in PBS containing 1% BSA, washed, counter-stained for 5 min with 0.1 mg/ml 4',6'-diamidino-2-phenyindole (DAPI) at room temperature and rinsed (5 times 3 min) with PBS. The sections were mounted in Gel Mount (Biomeda, Burlingame, CA). PBS-BSA 1% instead of the primary antibody was used as a negative control. Slides were examined with a fluorescent microscope Olympus IX70 coupled to a digital camera.

Terminal transferase dUTP nick end labeling: Tunel assay was carried out as previously described (Roche, Basel, Switzerland) [34]. Positive controls were obtained by inducing apoptosis with 1 µM staurosporine.

Cultures of rat retinal Müller glial cells and pigment epithelial cells: RMG and RPE cells were isolated under sterile conditions from Long Evans rats at postnatal (PN) day 8 to 12 as previously described [35]. Sub-confluent rat RPE and RMG cells were treated for 24 h with 1 or 0.1 mg/ml TA, dexamethasone (fluoromethylprednisolone; Dex), dexamethasone sodium phosphate (Dex-p), or hydrocortisone (Hyd-c). These compound were added directly to the culture medium. The effect of polysorbate 80 (FlukaSigma Saint-Quentin, Fallavier, France; 0.02, 0.2, and 2 mg/ml), the excipient in Kenacort Retard® preparation was also evaluated. Untreated cell cultures were used as controls.

Human ARPE-19 cells: Confluent ARPE-19 cultured cells were treated for 24 h with 0.1 and 1 mg/ml TA, dissolved or not in medium containing 1% ethanol (TA-eth) and Kenacort Retard® (Ken). Cells were also treated with Dexamethasone (Dex), Dexamethasone phosphate (Dex-p), or Hydrocortisone (Hyd-c) in medium containing 1% ethanol, or with polysorbate 80 (0.02, 0.2, and 2 mg/ml). Control cells were either untreated or treated with 1% ethanol.

Analysis of glucocorticoids effects on cultured cells: Cell viability: Viability was assessed by the tetrazolium 3-(4,5-dimethylthiazol-2-yl)-2,5 phenyltetrazolium bromide test (MTT) (Sigma Chemical, Saint Louis, CO) using 100.000 cells per well in 24 wells plates. Briefly, culture medium was removed and 250 µl of MTT (1 mg/ml in PBS) were added to each well, incubated for 1 h at 37 °C, lysed with 250 µl of isopropanol and assessed by measuring absorption at 570 nm versus 630 nm using a microplate reader (BioRad, San Diego, CA). Using a standard curve for each experiment, the color intensity observed in each well was correlated to the number of viable cells assessed by the trypan blue exclusion assay.

Evaluation of TA-induced cell death mechanism: ARPE-19 cells were seeded on round cover slides introduced at the bottom of 24 wells plates ($2x10^4$ cells/well) and grown at 37 °C in a humidified atmosphere containing 5% CO_2 and 95% air. Sub confluent cells were treated with 0.1 mg/ml TA or TA

in 1% ethanol. Control cells were run using the culture medium alone or the culture medium containing 1% ethanol. All experiments were performed in triplicates and repeated twice.

Immunocytochemistry: Cell staining using the following antibodies was carried out as specifically described [30-33,36-38]:

Polyclonal L-DNase II antibody [30,31] diluted (1/100) in PBS containing 1% skimmed milk.

Anti-Apoptosis-inducing factor (AIF) [36,37] (Sigma, Saint-Quentin Fallavier, France) diluted (1/100) in PBS containing 1% BSA.

Anti-Cytochrome C [38] (Sigma) diluted (1/250) in PBS containing 1% BSA.

Anti microtubules-associated protein and light chain 3 (MAP-LC3) [32,33] diluted (1/50) in PBS containing 1% fatty free milk.

After incubation with the specific primary antibodies, the cells were rinsed (3 times, 5 min each) with PBS, and then incubated for 1 h with goat Alexa Fluor anti-rabbit IgG (Molecular Probe Invitrogen, NY) diluted (1/250) in PBS containing 1% BSA, rabbit anti-goat texas red dye-conjugated (Jackson Immuno research laboratories INC) and chicken IGY-FITC conjugate (Promega) for 1 h, then washed in PBS (5 times, 5 min each). Positive controls for L-DNase II and AIF were obtained by inducing apoptosis with HMA (Hexa-methylene amiloride; Sigma) at 40 μM for 24 h. Positive controls for LC3 were obtained by culture in an amino acid depleted medium for LC3. Positive controls for apoptosis were obtained by inducing cell death with 1 μM staurosporine.

Western-blot analysis: Total ARPE-19 cell extracts were obtained by collecting the cells at the end of the treatment period and lysed in Laemmli sample buffer. Extracted proteins were separated by SDS-PAGE, immobilized on nitrocellulose membrane (Millipore, Billerica, Billerica, MA) and blotted with:

Rabbit polyclonal anti-caspase-3 antibody (Santa Cruz Biotechnology, Santa Cruz, CA) in a 1:800 dilution

Affinity purified rabbit anti-active Caspase-3 polyclonal antibody in a 1:500 dilution (Calbiochem, San Diego, CA)

Rabbit polyclonal anti-JNK1 (Santa Cruz Biotechnology, Santa Cruz, CA) in a 1:500 dilution

Rabbit polyclonal anti-active JNK pAb (Santa Cruz Biotechnology) in a 1:1000 dilution

The secondary goat-anti-rabbit IgG and rabbit anti goat IgG antibodies (Vector Laboratories, Burlingame, CA) were used in a 1/5000 and 1/10000 dilution. The amount of total protein extracts analysed was 30 μg/lane. Positive controls for caspase 3 activation were run on HL-60 cells treated for 24 h with 50 μM etoposide [39].

Lactate dehydrogenase cytotoxicity assay: ARPE-19 cells were seeded in 24 wells cell culture plates. Sub confluent cells were treated with TA (1 and 0.1 mg/ml), TA/ethanol (1 and 0.1 mg/ml, 1% ethanol/ml), Polysorbate 80 (2, 0.2, and 0.02 mg/ml) or Triton (0.2%) for 24 h. Released LDH in culture supernatants was measured using Cytotoxicity Detection Kit (Roche Applied Science). Dye absorbance was measured at 490 nm using a standard ELISA plate reader.

Vacuoles staining using monodansylcadaverine: Detection of monodansylcadaverine, a marker for autophagic vacuoles was performed as described [40]. Positive controls were run by incubating cells with an amino acid depleted medium (AAdep).

Evaluation of AIP-1/Alix transfection on triamcinolone acetonide-reduced cell viability: ARPE-19 cells were nucleofected using the cell line nucleofector kit V (Amaxa Bio systems, Cologne, Germany), with 2 μg of pCI mammalian expression vectors, empty or containing Alix-Wild type or its C-terminal moiety (a gift of Professor Remy Sadoul). Twenty-four h post nucleofection, the cells were treated by 0.1 mg/ml TA-1%ethanol. Cell viability was evaluated after 24 h of incubation using the MTT test as described above.

Transmission electron microscopy of cultured cells: For transmission electron microscopy (TEM), treated and control cells were washed in PBS, fixed with 2% glutaraldehyde for 30 min at room temperature, washed in 0.1 M cacodylate buffer pH 7.4 and post-fixed with 1% osmium tetroxyde for 15 min at room temperature. Cells were dehydrated in a graded series of ethanol (70-100 °C) and flat-embedded in Epon. Ultra-thin sections (70-80 nm) were obtained using an ultra-microtome (Reichert OM, UZ), counterstained with uranyl acetate and lead citrate and examined using an electron microscope (Philips CM10).

Statistical analyses: Statistical analyses were performed by computer (GraphPad Software Inc., San Diego, CA). Normality was tested with the Kolmogorov-Smirnov test. Differences between groups were compared by using the nonparametric Mann-Whitney test. Data are expressed as the mean±SD, and the differences was considered statistically significant at $p<0.05$.

RESULTS

Analysis of the rat retina after intra vitreous injection of Kenacort: In order to investigate the effects Kenacort® on rat retina, 1 μl (40 mg/ml) was injected into the vitreous. An equal volume of PBS was injected in control eyes and microscopic analysis was performed on semi-thin sections. After PBS injection, no structural changes were observed at 24 h and 8 days (Figure 1A). In eyes receiving Kenacort®, while no detectable anatomical changes were detected after 24 h (not shown), marked morphological changes in RPE cells and photoreceptors outer and inner segments were detected at 8 days (Figure 1B,C). At this time point, the photoreceptors outer segments were disorganized but the cell bodies remained relatively preserved. No cell gaps were detected in the RPE layer. However, the individual RPE cells were enlarged, demonstrated various sized cytoplasm vacuoles and increased microvilli (Figure 1B,C, short arrows). This morphological aspect suggested that replacement of lost RPE cells by enlargement of neighboring cells is taking place.

TEM observations correlated well with the changes observed on semi-thin sections. Figure 1D represents normal RPE cells from a PBS injected eye. In Kenacort ® treated eyes, the RPE cells cytoplasm was filled with vacuoles which were membrane-limited and contained cellular debris (Figure 1E,

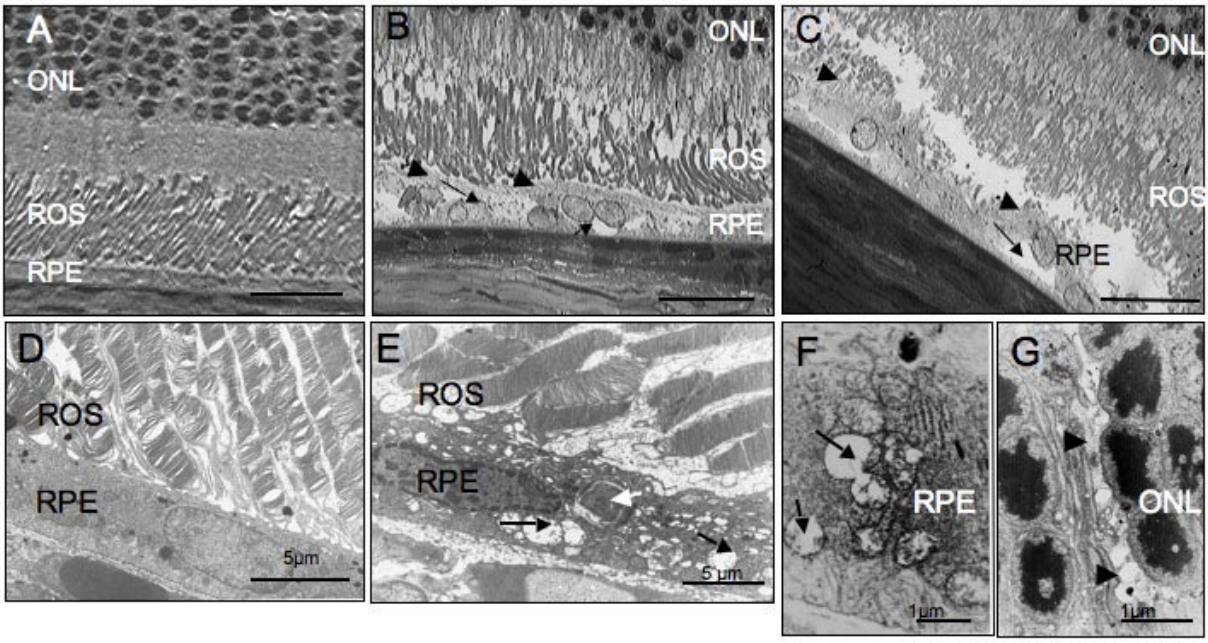

Figure 1. Structural alterations of the rat retina 8 days after intravitreous injection of Kenacort. **A**: Retina from a PBS-treated rat (control). **B**, **C**: Retina from Kenacort®-injected eyes. Thin black arrows show vacuoles and enlarged retinal pigment epithelium (RPE) cells. Thick arrows indicate increased RPE microvilli length. Scale bar represents 10 µm. Lower panels are ultrathin sections. **D**: Retina from a PBS-treated rat (control). **E**, **F**, **G**: Retina from Kenacort®-injected eyes. **E**: RPE cells show cytosolic vacuoles and dilated mitochondria (black arrows), as well as undigested debris (white arrow). A higher magnification of degraded mitochondria is shown on **F** (arrows). **G**: Vacuoles (arrows) are also observed in retina glial Müller cells prolongations. Note preservation of photoreceptor nuclei. ROS indicates rod outer segments, ONL indicates outer nuclear layer.

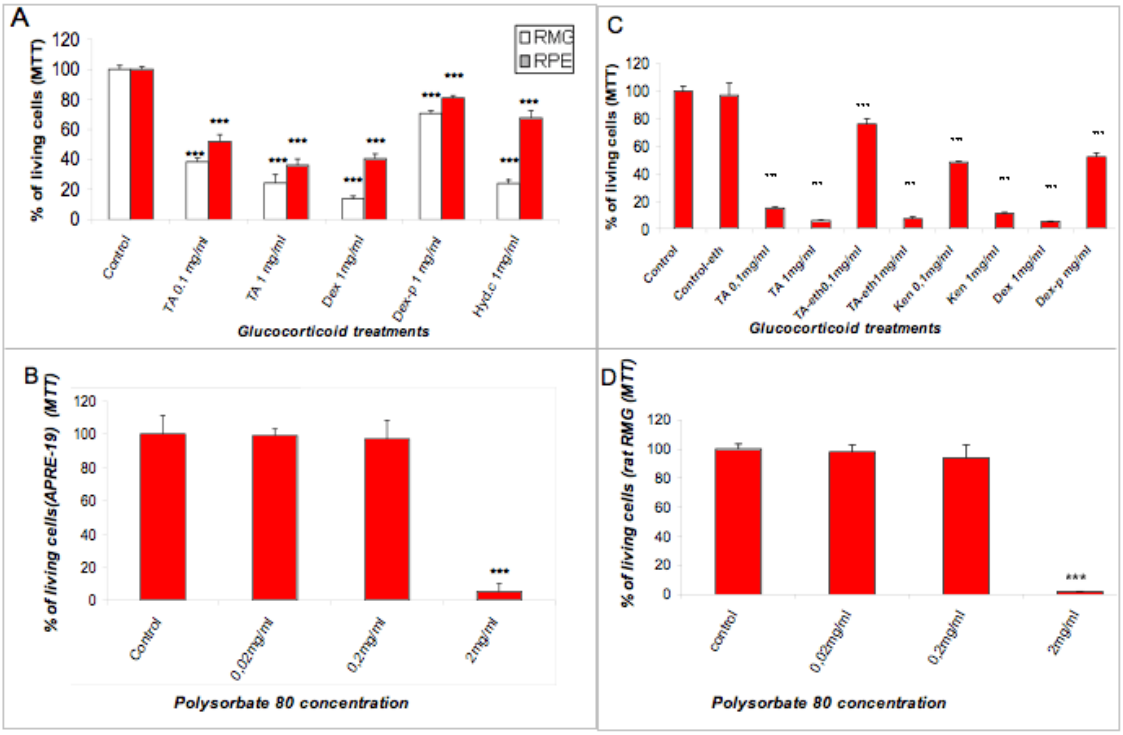

Figure 2. Effect of different glucocorticoids and polysorbate 80 on rat retinal pigment epithelium and retinal Müller glial and on human ARPE-19 cell survival. **A**, **B**: Primary culture of rat retinal Müller glial (RMG; white bars) or retinal pigment epithelium (RPE; grey bars) cells. **C**, **D**: Subconfluent ARPE-19 cells. The rate of survival was measured with the 3-(4,5-dimethylthiazol-2-yl)-2,5 phenyltetrazolium bromide test assay. TA represents triamcinolone, ken represents kenacort®, Dex represents dexamethasone, Dex-p represents dexamethasone sodium phosphate. Asterisk (*) indicates a $p<0.05$, double asterisk (**) a $p<0.01$, triple asterisk (***) a $p<0.001$.

arrows). These vacuoles appeared to be formed by confluent membranes of "empty" mitochondria (Figure 1F). The presence of large phagosomes was also seen (Figure 1E, white arrow). In some areas, cytoplasm elongated digitations were observed. Interestingly, vacuolization within the cytoplasm was also observed in RMG. In these cells, the vacuoles were mostly located within their prolongations in the outer nuclear layer (Figure 1G arrowheads). The photoreceptor nuclei, exhibited a normal morphology. These morphological changes indicated a cellular stress but they were not in agreement with an apoptotic form of cell death.

In order to verify if classical executors of apoptosis were activated, we immunostained cryosections from rats treated as before with anti-activated caspase 3. The control and Kenacort® treated eyes demonstrate similar patterns of staining for activated caspase 3, suggesting that caspase-dependent pathway is not activated (not shown). Same results were obtained when an anti-LEI/L-DNase II antibody was used (not shown) suggesting that this caspase independent apoptotic pathway, was not activated either. Finally, as the presence of multiple vacuoles may suggest activation of autophagy, we performed the same experiments using anti-LC3, a protein of the autophagic vesicles. Here again control and Kenacort® retinas presented similar immunostaining patterns.

Effect of corticosteroids on the viability of rat retinal macroglia Müller cells and retinal pigment epithelium cells in culture: In vivo studies suggested that RPE and Müller glial cells were affected by the intravitreous injection of Kenacort®. Viability of RPE and RMG cells was therefore evaluated in vitro in the presence of triamcinolone acetonide and other glucocorticoid chemical forms. As shown in Figure 2A, all tested corticosteroid formulations: Dexamethasone (Dex), dexamethasone sodium phosphate (Dex-p), TA, and hydrocortisone (Hyd-c) altered at various degrees the cell viability. RMG cells were more sensitive than RPE cells to the presence of all glucocorticoids in the culture medium. TA induced a dose-dependent reduction in cell viability with the loss of about 50% of living cells at 0.1 mg/ml. The reduced viability measured by the MTT assay was correlated to a reduced number of living cells as counted using the trypan blue assay. Dex and TA induced a higher toxic effect while Hydro-c and Dex-p were less toxic, particularly on RPE cells. This differential toxicity was less striking on RMG cells. The reduction in cell viability was associated with the chemical properties of the compounds: the more hydrosoluble formulation was correlated to a weaker toxicity. This was mostly evident when the different dexam-

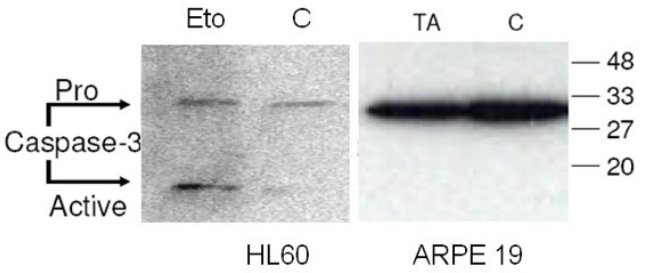

Figure 4. Absence of activation of caspase 3 in ARPE-19 cells. Subconfluent ARPE 19 cells were incubated for 72 h in the presence 0.1 mg/ml triamcinolone (in 1% ethanol). Protein extracts were separated in 4-10% PAGE, transferred to nitrocellulose and revealed with anti-caspase 3. No activation of caspases 3 is seen in TA-treated cells. Apoptosis induced in HL-60 with etoposide (50 μM for 24 h) was used as positive control.

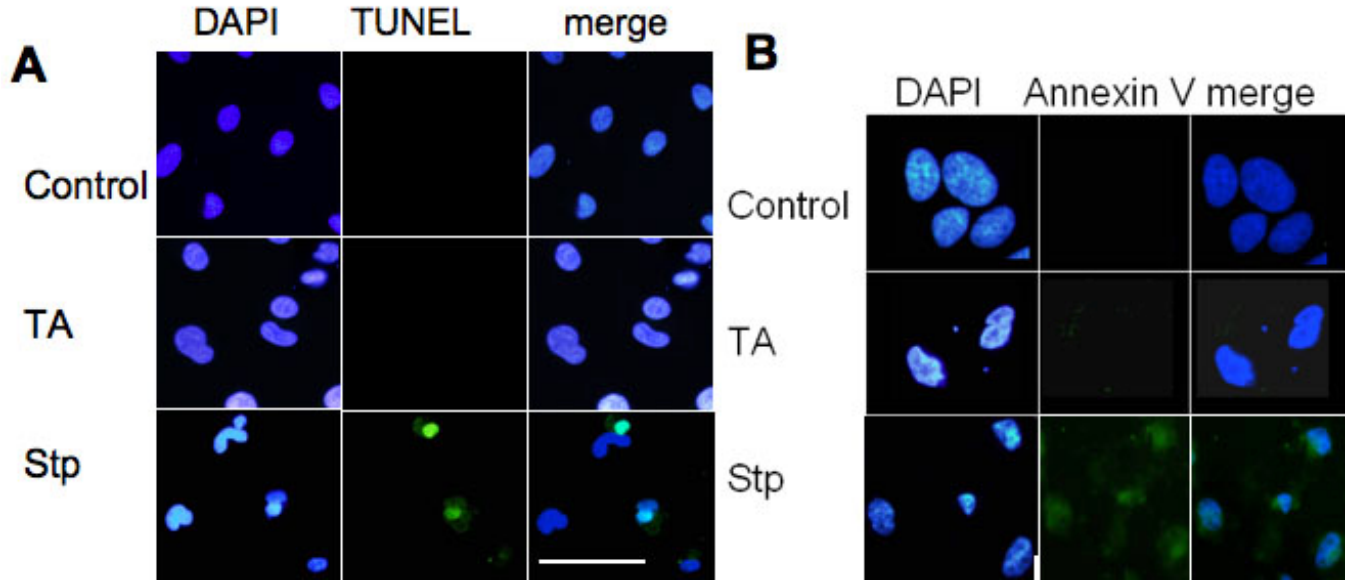

Figure 3. Absence of apoptosis markers in ARPE-19 cells treated with triamcinolone acetonide. Subconfluent ARPE 19 cells were incubated for 72 h in the presence triamcinolone (TA). Cells were then stained with TUNEL assay (**A**) or with annexin V (**B**). ARPE cells induced to die by treatment with 1 μM staurosporin (stp) for 24 h were used as positive controls (stp). Scale bar represents 50 μm.

ethasone preparations were used. Dex-p is less toxic than Dex.

Polysorbate 80, one of the Kenacort excipient significantly reduced both RPE and RMG cell viability, but only at the highest concentration tested (2 mg/ml). No significant toxicity was observed when 0.02 mg/ml (concentration in the Kenacort® preparation) and 0.2 mg/ml were used (Figure 2B).

We also observed that hydrophobic glucocorticoids added to the cell cultures without previous dispersion in ethanol formed dense and adherent aggregates that could not be removed by successive rinsing. These deposits on the cell surface interfered with histochemistry interpretation. All further analyses were therefore carried out with the glucocorticoids dissolved in medium containing 1% ethanol.

Effect of different triamcinolone acetonide formulations and polysorbate 80 on human ARPE-19 cell viability: Previous experiments indicated that glucocorticoids affect the viability of rat retinal cells. In order to further investigate the toxic mechanisms, we used ARPE19 cells, an established cell line derived from human RPE, which keeps differentiation markers in culture similar to those of primary human RPE cells.

First ARPE-19 viability was evaluated after treatment with TA. As expected, the solubilization of TA in ethanol reduced its toxicity (Figure 2C). Control cells treated with 1% ethanol, did not show any reduced viability. At a concentration of 0.1 mg/ml, 80% of the cells remained viable when the drug dissolved in ethanol was used while only 20% of the cells are viable when the insoluble TA powder is used. At the concentration of 1 mg/ml, only part of the TA is dissolved by the alcohol. Kenacort® toxicity is intermediate between TA in ethanol and TA in solution inducing a 50% cell death at 0.1 mg/ml. Toxicity of 1 mg/ml dexamethasone dissolved in ethanol was also dependent on the chemical form used with a much higher toxicity induced by the fluoromethyl than by the sodium phosphate form. These results showed again that the lower solubility and higher hydrophobic glucocorticoid forms are more toxic for the ARPE-19 cells. Figure 2C shows that polysorbate 80 at a concentration of 0.02 mg/ml (similar to that of the Kenacort® preparation) or even at a higher concentration of 0.2 mg/ml, did not influence ARPE-19 cell viability (Figure 2D).

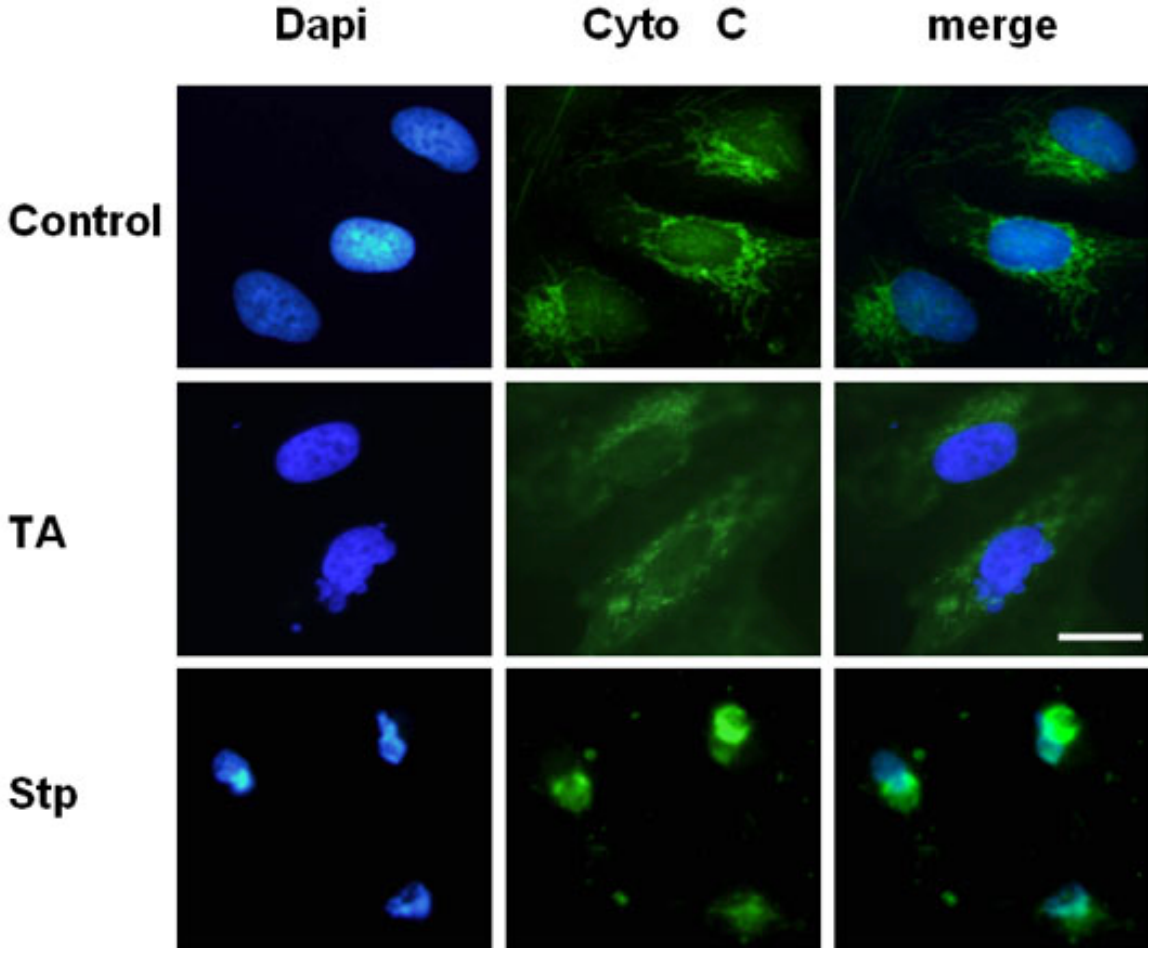

Figure 5. No release of cytochrome C from mitochondria in triamcinolone-treated-ARPE-19 cells. ARPE 19 cells cultured in the presence 0.1 mg/ml triamcinolone (in 1% ethanol) were immunostained with anti cytochrome C. Dotted disposition of staining in both control and TA treated cells indicate that this molecule remains in the mitochondria. Apoptosis induced in ARPE cells with staurosporine was used as positive control. Scale bar represents 10 μm.

Apoptosis in triamcinolone acetonide associated toxicity: Caspase-dependent apoptosis was often associated with a positive TUNEL staining. No TUNEL positive ARPE-19 cells could be detected after treatment with TA/ethanol (Figure 3A, TA) or in control ethanol treated cultures (Figure 3A, Control) In addition, annexin-V did not bind to ARPE-19 cells exposed to TA (Figure 3B) indicating that no exposition of phosphatidylserine is induced. On the contrary, Cells treated with staurosporine (Stp), a well know apoptosis inducer were TUNEL and annexin positive (Figure 3A,B, Stp). Other biochemical markers of apoptosis were also negative. No activated caspase-3 was detected (Figure 4) in any of the TA-treated or control cultures suggesting that caspase-3 cleavage did not occur. In addition, cytochome C cell localization was similar in cell cultures exposed to TA and in negative controls (Figure 5). Thus, release of cytochrome C from mitochondria, a major event during apoptosis, did not occur in TA-treated cells but occurred in Stp treated cells (Figure 5, Stp). These data excluded caspase-dependent apoptosis as a potential mechanism for the observed cell death induced by the corticosteroids.

Two markers of caspase-independent apoptosis were also investigated: LE/L-DNase II and AIF (Apoptosis inducing factor). LEI/L-DNase II antibody recognizes both the leucocyte elastase inhibitor (LEI) and the L-DNase II forms of this protein. Nuclearization of the signal detects the cleavage of LEI into L-DNase II [30,31] and the activation of this non-caspase apoptotic pathway in cell death. In the same way, when translocated into cell nuclei, AIF is a marker of caspase-independent. apoptosis AIF and LEI were observed within the cytoplasm of the cells but did not undergo nuclear translocation after TA treatment (Figure 6A). In cells treated with HMA, a known inducer of non-caspase apoptosis, both LEI and AIF did translocate into the nucleus of ARPE-19 cells (Figure 6B).

Necrosis: TA-induced cell death lacked the specific markers and morphology for apoptotic cell death. To investigate the possibility of a passive cell death, e.g. necrosis, we measured the amount of free LDH in the various types of cell cultures. Table 1 shows the absence of necrosis with 0.1 mg/ml TA in 0.1%/ethanol. Nonetheless, higher TA concentrations as well as addition of the more hydrophobic glucocoticoid compounds induced a measurable LDH release. These results could indicate that at high concentrations, a fraction of the corticosteroid-induced toxicity may be driven by necrosis. However they also indicated the presence of another cell death mechanism, as the percentage of dead cells is always higher than the percentage of necrotic cells.

Autophagy and paraptosis: Autophagic activity was investigated by vacuoles labeling using both monodansylcadaverine and anti-LC3, an antibody staining mature autophagic vacuoles [33].

Only some of the vacuoles were stained with monodansylcadaverine in TA-treated RPE cells (Figure 7A, arrowheads), while larger vacuoles inducing a modification of the cell nucleus shape (Figure 7A,D arrowheads) were not stained. MAP-LC3 labeling did not significantly differ in TA treated and control cells, while MAP-LC3 positively stained vacuoles of cells incubated in amino acid depleted medium (AAdep, Figure 7).

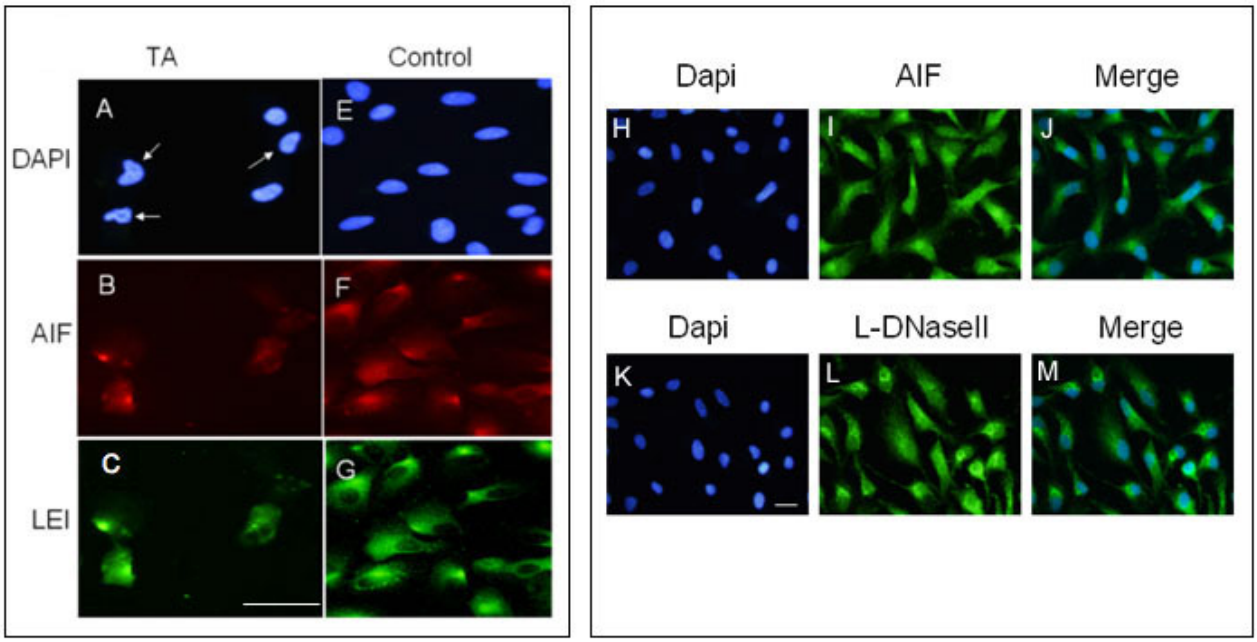

Figure 6. No caspase-independent markers of apoptosis in triamcinolone treated ARPE-19 cells. **A**- **G**: Triamcinolone-treated (0.1 mg/ml in 1% ethanol) or control ARPE 19 cells were stained with DAPI or immunostained with anti-AIF or anti LEI/L-DNase II. No nuclear translocation of these apoptosis markers was seen, neither in cells with normal morphology, nor in cells with an altered nuclear morphology (**A**, white arrows). **H**-**M**: Induction of apoptosis with HMA was used as positive control and shows nuclear translocation of both LEI and AIF, both markers of caspase independent apoptosis. Sacle bar represents 20 μm.

TEM morphology analysis showed that ARPE-19 control cells (PBS treated) did not show any signs of stress and the mitochondria are well preserved (Figure 8A). On the other hand, 0.1 mg/ml TA-treated ARPE-19 showed cytoplasm vacuolization and alterations of the mitochondria (Figure 8B, arrows) associated with a dilatation of the endoplasmic reticulum (Figure 9B arrowheads). More intense cell vacuolization, a loss of normal mitochondria and the presence of electron dense debris (arrows) were observed in cells exposed to 1 mg/ml TA (Figure 8C). Noteworthy is the fact that the chromatin in these cultured cells has a normal aspect. TEM morphologic changes were mostly suggestive of paraptosis.

To further investigate this possibility, we studied the phosphorylation of JNK and the effect of Alix over expression (both wild type and the C terminal fragment) in cultured cells since the inhibition by AIP-1/Alix can be considered as specific for paraptosis [28].

As shown in Figure 9A, over-expression of AIP-1/Alix in ARPE-19 cells significantly reduced TA-induced toxicity (0.1 mg/ml in 1% ethanol). Only 8% of cell death was ob-

Table 1. Lactate dehydrogenase release in ARPE-19 cells

Treatment	LDH release (%)	Estimated dead cells (%)
TA 0.1 mg/ml	52	85
TA 1 mg/ml	52	94
TA 0.1 mg/ml-eth	0	24
TA 1 mg/ml-eth	52	92
Kenacort 0.1 mg/ml	20	51
Kenacort 1 mg/ml	47	84
Dexa 0.1 mg/ml-eth	0	48
Dexa 1 mg/ml-eth	65	94

The release of lactate dehydrogenase (LDH) from ARPE-19 cells treated with different corticoid at different concentrations was measured in the culture medium and compared with the total amount of LDH in these cells measured after an experimental lysis of parallel cultures (percent of LDH release). The second column represents the total cell death as measured by 3-(4,5-dimethylthiazol-2-yl)-2,5 phenyltetrazolium bromide test.

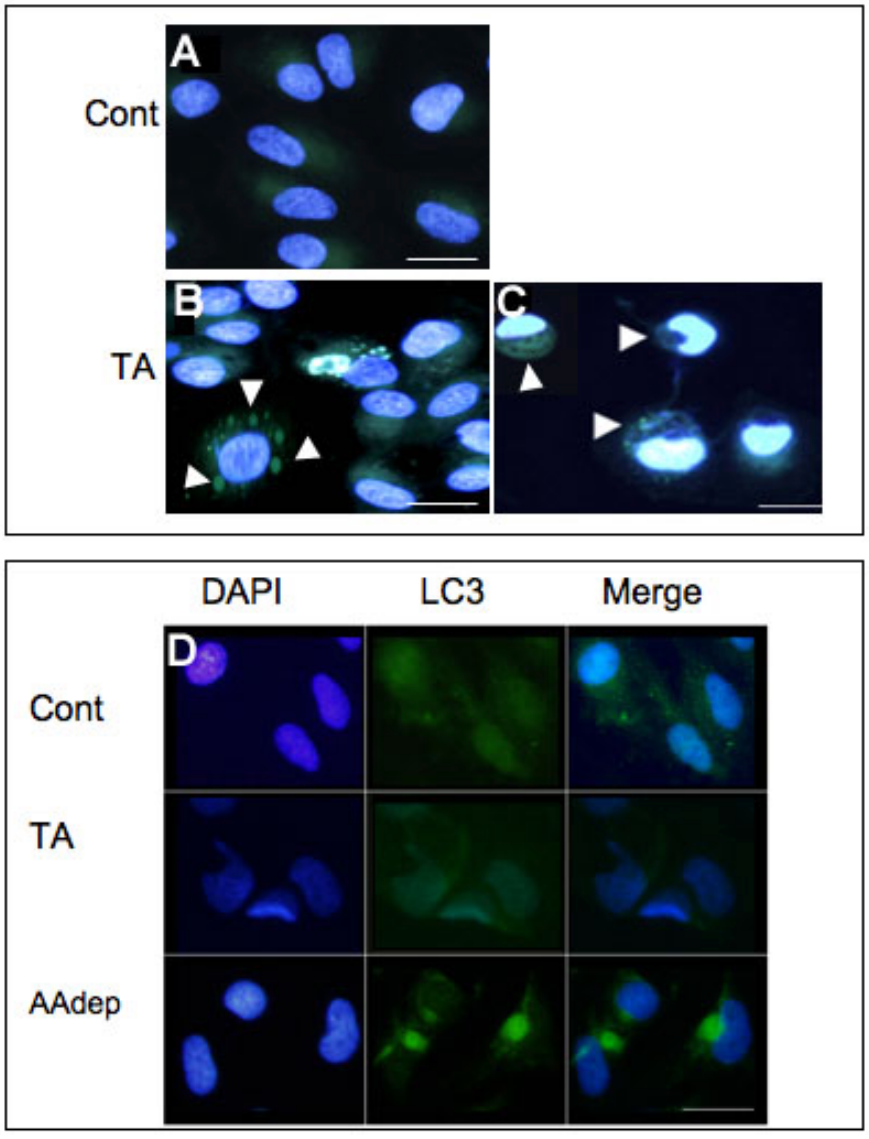

Figure 7. Markers of autophagy in triamcinolone treated ARPE-19 cells. **A**-**C**: Monodansylcadaverine staining in control (**A**) and 0.1 mg/ml (in 1% ethanol) TA-treated ARPE-19 cells (**B** and **C**). Small monodansylcadaverine positive (**B**) vesicles (white arrowheads), and larger vesicles not stained with monodansylcadaverine (**C**) are observed in TA-treated cells. **D**: An anti-LC3 immunostaining in control (**A**) and TA-treated ARPE-19 cells (**B**), and in cells treated with cells an amino acid deplete medium (AA dep; **C**). LC3 is evenly distributed in control and TA-treated cells. In cells treated with AAdep, LC3 is concentrated in autophagic vesicles. Scale bar represents 20 μm.

served in AIP-1/Alix-WT transfected cells as compared to 23% in non-transfected cells or in cells transfected with wild type AIP-1/Alix-CT (Figure 9A). Thus, the over-expression of Alix-WT was associated with a significant protection against TA-induced cell death. Activation of JNK-1 and JNK-2 was investigated using anti-phospho JNK antibodies. TA induced phosphorylation of a 57 kDa protein that may correspond to JNK-2 but did not demonstrate an increase in JNK-1 phosphorylation (Figure 9B).

DISCUSSION

Contradictory observations and discrepancies regarding the clinical safety of intravitreous TA and the in vitro TA-induced toxicity have been published [12,17], depending mostly on the techniques used to detect toxicity. In the rat eye, using semi-thin histology and TEM 8 days after the intravitreous injection of Kenacort®, we can detect clear lesions in RPE and macroglial cells. These morphological abnormalities are not associated with infiltration of inflammatory cells, or with glial activation (no GFAP labeling is found, not shown). Recently, TEM analysis of the rabbit retina after the intravitreous injection of Kenalog®, showed the same lesions [41]. The fact that all currently used immunohistochemical markers for apoptosis or autophagy (activated caspase-3, TUNEL assay, and MAP-LCA) are negative may explain why other authors previously failed to detect any toxic effects in the rabbit eye [12,14].

Our in vitro studies confirm that glucocorticoids have a toxic effect on rat RPE and RMG cells and on human ARPE-19 cells. A significant and dose dependent toxicity was induced by different glucocorticoid formulations. The chemical properties of the glucocorticoids determine their toxicity: more hydrophobic compounds induce a more toxic effect. Dex and TA demonstrate the highest toxic effect while Hydro-c and Dex-p are less toxic. This phenomenon may be associated with the lesser ability of the cells to metabolize the hydrophobic compounds allowing for their accumulation and higher concentration in the cell and intracellular organ membranes.

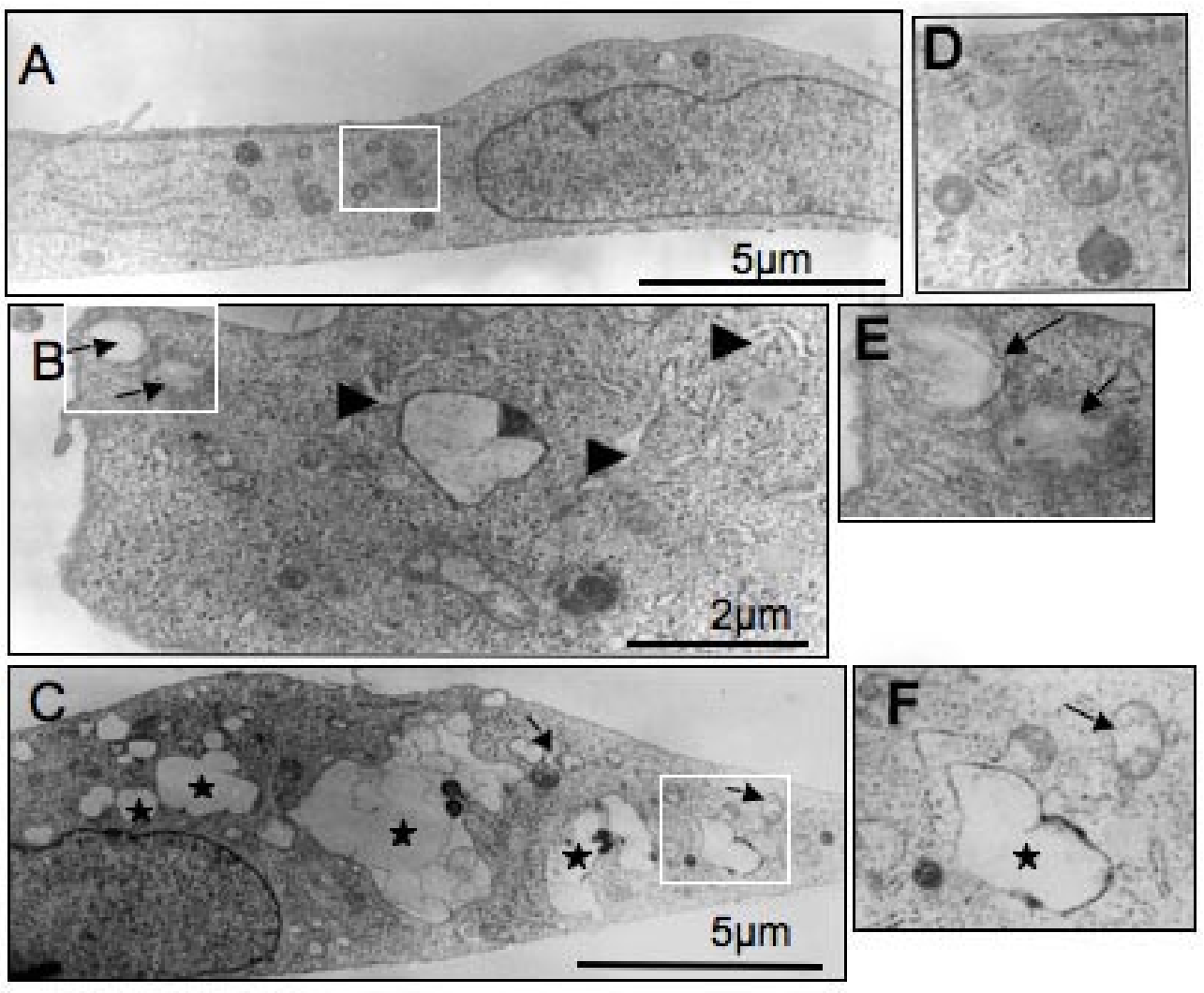

Figure 8. Transmission electron microscopyobservations of TA-treated ARPE 19 cells. **A**: Control ARPE 19 cells. **B** and **C**: ARPE-19 cells TA-treated with 0.1 mg/ml (**B**) and 1 mg/ml TA (**C**), showing membrane limited (arrows) or unlimited vesicles (stars) and dilated endoplasmic reticulum (arrowhead). In picture **C**, a more advanced stage of degeneration is represented.

Kenacort®, commonly used for clinical use contains two phases: crystals of TA in suspension and a low fraction of TA solubilized in polysorbate 80 (0.02 mg/ml) and benzyl alcohol. Polysorbate 80 is an anionic detergent of low toxicity [42] which can however, increase susceptibility to oxidative stress [43]. When cells are exposed in vitro to polysorbate 80 at concentrations of 0.02 mg/ml no toxicity is observed. These results indicate that polysorbate 80 per se is not toxic. Others authors have reported that Kenalog® vehicle enhance the toxicity of TA on retinal cells in culture [17]. Indeed, in contrast to polysorbate 80, benzyl alcohol (contained in Kenalog®) induce ARPE-19 apoptosis, even at low concentrations [18]. Therefore, it was recommended to remove the solubilizing compounds within the Kenalog® preparation before its injection in the human eye [19,44]. However, the potential toxic effect of the TA crystals was somewhat overlooked.

From our present study, it can be concluded that an important part of the TA toxicity is associated with the low solubility of the compound. The cell toxicity of 0.1 mg/ml TA in 1% ethanol was significantly reduced when compared to the same concentration of TA in crystal form. At the concentration of 1 mg/ml TA, the use of 1% ethanol did not influence the extent of cell toxicity because a large proportion of the TA crystals still remain insoluble. Similarly, it was recently shown that direct contact of insoluble TA with ARPE-19 cells induced cell death through an apopto-necrotic mechanism [18]. Previous in vitro experiments have also shown that direct incubation of cells with crystalline TA induce activation of caspases and stress proteins [15]. On the other hand, when TA crystals are separated from the ARPE-19 cultured cells by a microporous membrane, no apoptotic cell death occurred [18]. However, in these experiments, other potential mechanisms of cell death, different from apoptosis were not explored.

In the brain, it was reported that the glucocorticoid II receptor mediates cell toxicity [45] and in hyppocampal neurons, corticosterone neurotoxicity has been correlated to alteration of the mitochondrial membrane potential. Interestingly, in these studies, no apoptosis markers could be detected and the exact mechanism of cell death remains elusive [46].

Although corticosteroids significantly reduce the number of living cells, we failed to observe any significant activation of the known apoptotic pathways in retinal cells, which is in line with previous reports indicating the failure to detect evident apoptosis during RPE cell death induced by corticosteroids [15,17]. Our further exploration of other types of programmed cell death sheds light on the possible mechanisms of retinal cell death pathways activated by the corticosteroids.

The extensive vacuolization within the cytoplasm and deformation of the nucleus shape and contour in TA treated cells could suggest potential an autophagic mechanism, which is characterized by sequestration of bulk cytoplasm and the formation of organelles in double or multimembrane acidic autophagic vesicles [23,25]. During autophagy, a specific form of the microtubule -associated protein light chain 3 (LC3), the LC3-2 form has been described to increase in association with the autophagosome membrane [31,32]. This reaction seems however not to be specific for autophagy [32,39]. In our study, using both immunostaining and western blotting (not shown), we did not find any evidence for LC3 association with the observed vacuoles and could not detect any increase of LC3-2 in TA treated cells. This did not favor the hypothesis of autophagy. Interestingly, in neural cells, the suppression of basal autophagy may rather cause neurodegeneration [47,48].

However, the observation that in some TA treated cells, vesicles positive for monodansylsacaderine were detected does not allow to totally ruled out the possibility that autophagy can be part of the mechanisms involved in TA induced cell death.

TEM observations of retina and cells treated with TA showed that the large irregular cytoplasmic vacuoles are associated with swelling of the mitochondria and enlargement of the endoplasmic reticulum along with preservation of the nuclear chromatin, which may suggest paraptotic cell death [27,29]. Paraptosis takes place during cell differentiation in the development of the nervous system as well as in some cases of neurodegeneration [22]. It is mediated by mitogen-activated protein kinases and can be triggered by the TNF re-

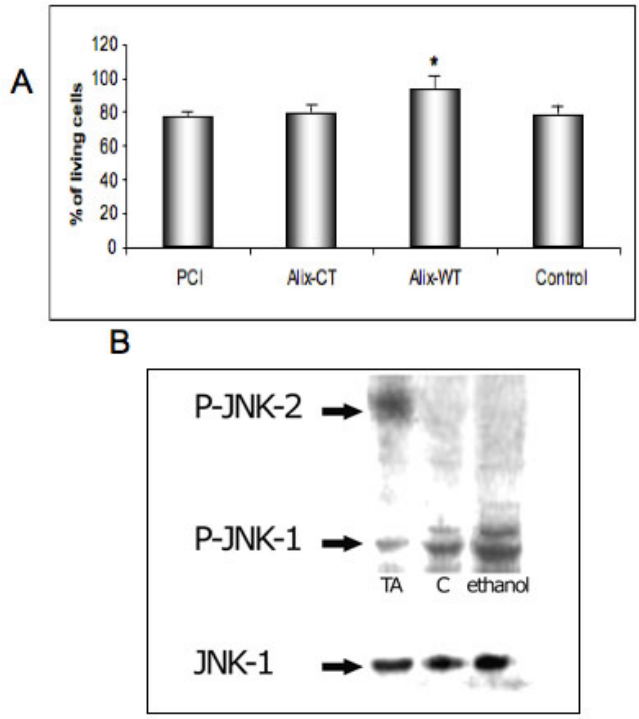

Figure 9. Paraptosis in triamcinolone treated-ARPE-19 cells. **A**: Effect of Alix overexpression on TA induced cell death. ARPE 19 cells were nucleofected with Alix-WT or with its C terminal moiety. Controls were run with untransfected cells or in cells transfected with the PCI empty vector. 48 h after transfection cells were treated with TA and cell survival was measured with the 3-(4,5-dimethylthiazol-2-yl)-2,5 phenyltetrazolium bromide test method. Alix-CT has no effect on cell survival but Alix-WT protects cells form death. * indicates a $p<0.05$. **B**: Western-blot using anti-PJNK (upper panel) or anti-JNK-1 (lower panel) was assayed in 0.1 mg/ml (in 1% ethanol) TA treated (TA) or control (**C**, 1% ethanol) ARPE-19 cells. An increase of P-JNK-2 is seen in TA treated cells, while no JNK-1 over activation is observed in TA-treated cells compared to control cells.

ceptor family member TAJ/TROY [29]. The fact that ARPE-19 cells TA-induced toxicity can be blocked by the paraptosis inhibitor AIP-1/Alix, but not with its anti-apoptotic C-terminal fragment (Alix-CT), favors further the hypothesis of paraptosis [28]. It was recently shown that in insulin-like growth factor I receptor (IGFIR)-induced paraptosis the MEK/JNK-1 pathway was involved [28]. In TA-induced paraptosis of ARPE-19 cells, we found that phosphorylation of JNK-2 occurs but no phosphorylation of JNK-1. This situation has already been described for other cells [49].

Taken together, our observations suggest that non classical mechanisms of cell death are induced by the corticosteroids. Apparently, the activated specific mechanism depends on the formulation of the used compounds and involves different mechanisms of cell death. The presence of insoluble particles induces mostly a necrotic response. In the presence of soluble formulations of TA, which is studied in this work, the major cell death mechanism is related to paraptosis.

In conclusion, we demonstrate that glucocorticoids induce non-apoptotic cell death through a mechanism related mainly to paraptosis. Whether glucocorticoids can induce similar toxic effects in other cell types remain to be investigated, but the failure to detect apoptotic markers in other neural cells favor this hypothesis. These observations enhance our understanding of the glucocorticoid mechanism of action on ocular tissues and open the way for the investigations of more efficient and safer future therapeutic avenues.

ACKNOWLEDGEMENTS

We are greatly indebted to Prof. R. Sadoul and Dr. C. Chatellard-Cause (EMI 0108, LAPSEN, Grenoble, France) for the generous gift of Alix and Alix-CT plasmids.

REFERENCES

1. Jonas JB, Hayler JK, Sofker A, Panda-Jonas S. Intravitreal injection of crystalline cortisone as adjunctive treatment of proliferative diabetic retinopathy. Am J Ophthalmol 2001; 131:468-71.
2. Jonas JB, Kamppeter BA, Harder B, Vossmerbaeumer U, Sauder G, Spandau UH. Intravitreal triamcinolone acetonide for diabetic macular edema: a prospective, randomized study. J Ocul Pharmacol Ther 2006; 22:200-7.
3. Martidis A, Duker JS, Greenberg PB, Rogers AH, Puliafito CA, Reichel E, Baumal C. Intravitreal triamcinolone for refractory diabetic macular edema. Ophthalmology 2002; 109:920-7.
4. Greenberg PB, Martidis A, Rogers AH, Duker JS, Reichel E. Intravitreal triamcinolone acetonide for macular oedema due to central retinal vein occlusion. Br J Ophthalmol 2002; 86:247-8.
5. Antcliff RJ, Spalton DJ, Stanford MR, Graham EM, ffytche TJ, Marshall J. Intravitreal triamcinolone for uveitic cystoid macular edema: an optical coherence tomography study. Ophthalmology 2001; 108:765-72.
6. Munir WM, Pulido JS, Sharma MC, Buerk BM. Intravitreal triamcinolone for treatment of complicated proliferative diabetic retinopathy and proliferative vitreoretinopathy. Can J Ophthalmol 2005; 40:598-604.
7. Young S, Larkin G, Branley M, Lightman S. Safety and efficacy of intravitreal triamcinolone for cystoid macular oedema in uveitis. Clin Experiment Ophthalmol 2001; 29:2-6.
8. Challa JK, Gillies MC, Penfold PL, Gyory JF, Hunyor AB, Billson FA. Exudative macular degeneration and intravitreal triamcinolone: 18 month follow up. Aust N Z J Ophthalmol 1998; 26:277-81.
9. Danis RP, Ciulla TA, Pratt LM, Anliker W. Intravitreal triamcinolone acetonide in exudative age-related macular degeneration. Retina 2000; 20:244-50.
10. Ciulla TA, Criswell MH, Danis RP, Hill TE. Intravitreal triamcinolone acetonide inhibits choroidal neovascularization in a laser-treated rat model. Arch Ophthalmol 2001; 119:399-404.
11. Beer PM, Bakri SJ, Singh RJ, Liu W, Peters GB 3rd, Miller M. Intraocular concentration and pharmacokinetics of triamcinolone acetonide after a single intravitreal injection. Ophthalmology 2003; 110:681-6.
12. McCuen BW 2nd, Bessler M, Tano Y, Chandler D, Machemer R. The lack of toxicity of intravitreally administered triamcinolone acetonide. Am J Ophthalmol 1981; 91:785-8.
13. Kivilcim M, Peyman GA, El-Dessouky ES, Kazi AA, Cheema R, Hegazy H. Retinal toxicity of triamcinolone acetonide in silicone-filled eyes. Ophthalmic Surg Lasers 2000; 31:474-8.
14. Dierks D, Lei B, Zhang K, Hainsworth DP. Electroretinographic effects of an intravitreal injection of triamcinolone in rabbit retina. Arch Ophthalmol 2005; 123:1563-9.
15. Yeung CK, Chan KP, Chiang SW, Pang CP, Lam DS. The toxic and stress responses of cultured human retinal pigment epithelium (ARPE19) and human glial cells (SVG) in the presence of triamcinolone. Invest Ophthalmol Vis Sci 2003; 44:5293-300.
16. Yeung CK, Chan KP, Chan CK, Pang CP, Lam DS. Cytotoxicity of triamcinolone on cultured human retinal pigment epithelial cells: comparison with dexamethasone and hydrocortisone. Jpn J Ophthalmol 2004; 48:236-42.
17. Narayanan R, Mungcal JK, Kenney MC, Seigel GM, Kuppermann BD. Toxicity of triamcinolone acetonide on retinal neurosensory and pigment epithelial cells. Invest Ophthalmol Vis Sci 2006; 47:722-8.
18. Szurman P, Kaczmarek R, Spitzer MS, Jaissle GB, Decker P, Grisanti S, Henke-Fahle S, Aisenbrey S, Bartz-Schmidt KU. Differential toxic effect of dissolved triamcinolone and its crystalline deposits on cultured human retinal pigment epithelium (ARPE19) cells. Exp Eye Res 2006; 83:584-92.
19. Kai W, Yanrong J, Xiaoxin L. Vehicle of triamcinolone acetonide is associated with retinal toxicity and transient increase of lens density. Graefes Arch Clin Exp Ophthalmol 2006; 244:1152-9.
20. Lockshin RA, Zakeri Z. Apoptosis, autophagy, and more. Int J Biochem Cell Biol 2004; 36:2405-19.
21. Siegel RM. Caspases at the crossroads of immune-cell life and death. Nat Rev Immunol 2006; 6:308-17.
22. Broker LE, Kruyt FA, Giaccone G. Cell death independent of caspases: a review. Clin Cancer Res 2005; 11:3155-62.
23. Heymann D. Autophagy: A protective mechanism in response to stress and inflammation. Curr Opin Investig Drugs 2006; 7:443-50.
24. Yu L, Wan F, Dutta S, Welsh S, Liu Z, Freundt E, Baehrecke EH, Lenardo M. Autophagic programmed cell death by selective catalase degradation. Proc Natl Acad Sci U S A 2006; 103:4952-7.
25. Kelekar A. Autophagy. Ann N Y Acad Sci 2005; 1066:259-71.
26. Fietta P. Many ways to die: passive and active cell death styles. Riv Biol 2006; 99:69-83.
27. Fombonne J, Padron L, Enjalbert A, Krantic S, Torriglia A. A novel paraptosis pathway involving LEI/L-DNaseII for EGF-induced cell death in somato-lactotrope pituitary cells. Apoptosis 2006; 11:367-75.

28. Sperandio S, Poksay K, de Belle I, Lafuente MJ, Liu B, Nasir J, Bredesen DE. Paraptosis: mediation by MAP kinases and inhibition by AIP-1/Alix. Cell Death Differ 2004; 11:1066-75.
29. Wang Y, Li X, Wang L, Ding P, Zhang Y, Han W, Ma D. An alternative form of paraptosis-like cell death, triggered by TAJ/TROY and enhanced by PDCD5 overexpression. J Cell Sci 2004; 117:1525-32.
30. Torriglia A, Chaudun E, Chany-Fournier F, Jeanny JC, Courtois Y, Counis MF. Involvement of DNase II in nuclear degeneration during lens cell differentiation. J Biol Chem 1995; 270:28579-85.
31. Altairac S, Zeggai S, Perani P, Courtois Y, Torriglia A. Apoptosis induced by Na+/H+ antiport inhibition activates the LEI/L-DNase II pathway. Cell Death Differ 2003; 10:548-57.
32. Tanida I, Tanida-Miyake E, Ueno T, Kominami E. The human homolog of Saccharomyces cerevisiae Apg7p is a Protein-activating enzyme for multiple substrates including human Apg12p, GATE-16, GABARAP, and MAP-LC3. J Biol Chem 2001; 276:1701-6.
33. Asanuma K, Tanida I, Shirato I, Ueno T, Takahara H, Nishitani T, Kominami E, Tomino Y. MAP-LC3, a promising autophagosomal marker, is processed during the differentiation and recovery of podocytes from PAN nephrosis. FASEB J 2003; 17:1165-7.
34. Bourges JL, Valamanesh F, Torriglia A, Jeanny JC, Savoldelli M, Renard G, BenEzra D, de Kozak Y, Behar-Cohen F. Cornea graft endothelial cells undergo apoptosis by way of an alternate (caspase-independent) pathway. Transplantation 2004; 78:316-23. Erratum in: Transplantation. 2005; 79:502.
35. Behar-Cohen FF, Thillaye-Goldenberg B, de Bizemont T, Savoldelli M, Chauvaud D, de Kozak Y. EIU in the rat promotes the potential of syngeneic retinal cells injected into the vitreous cavity to induce PVR. Invest Ophthalmol Vis Sci 2000; 41:3915-24.
36. Yasugi E, Kumagai T, Nishikawa Y, Okuma E, Saeki K, Oshima M, Susin SA, Kroemer G, Yuo A. Involvement of apoptosis-inducing factor during dolichyl monophosphate-induced apoptosis in U937 cells. FEBS Lett 2000; 480:197-200.
37. Daugas E, Susin SA, Zamzami N, Ferri KF, Irinopoulou T, Larochette N, Prevost MC, Leber B, Andrews D, Penninger J, Kroemer G. Mitochondrio-nuclear translocation of AIF in apoptosis and necrosis. FASEB J 2000; 14:729-39.
38. Nur-E-Kamal A, Gross SR, Pan Z, Balklava Z, Ma J, Liu LF. Nuclear translocation of cytochrome c during apoptosis. J Biol Chem 2004; 279:24911-4.
39. Gokhale P, Patel T, Morrison MJ, Vissers MC. The effect of intracellular ascorbate on the susceptibility of HL60 and Jurkat cells to chemotherapy agents. Apoptosis 2006; 11:1737-46.
40. Biederbick A, Kern HF, Elsasser HP. Monodansylcadaverine (MDC) is a specific in vivo marker for autophagic vacuoles. Eur J Cell Biol 1995; 66:3-14.
41. Yu SY, Damico FM, Viola F, D'Amico DJ, Young LH. Retinal toxicity of intravitreal triamcinolone acetonide: a morphological study. Retina 2006; 26:531-6.
42. Sellers RS, Antman M, Phillips J, Khan KN, Furst SM. Effects of miglyol 812 on rats after 4 weeks of gavage as compared with methylcellulose/tween 80. Drug Chem Toxicol 2005; 28:423-32.
43. Tatsuishi T, Oyama Y, Iwase K, Yamaguchi JY, Kobayashi M, Nishimura Y, Kanada A, Hirama S. Polysorbate 80 increases the susceptibility to oxidative stress in rat thymocytes. Toxicology 2005; 207:7-14.
44. Hernaez-Ortega MC, Soto-Pedre E. A simple and rapid method for purification of triamcinolone acetonide suspension for intravitreal injection. Ophthalmic Surg Lasers Imaging 2004; 35:350-1.
45. Liu Y, Imai H, Sadamatsu M, Tsunashima K, Kato N. Cytokines participate in neuronal death induced by trimethyltin in the rat hippocampus via type II glucocorticoid receptors. Neurosci Res 2005; 51:319-27.
46. Roy M, Sapolsky RM. The exacerbation of hippocampal excitotoxicity by glucocorticoids is not mediated by apoptosis. Neuroendocrinology 2003; 77:24-31.
47. Komatsu M, Waguri S, Chiba T, Murata S, Iwata J, Tanida I, Ueno T, Koike M, Uchiyama Y, Kominami E, Tanaka K. Loss of autophagy in the central nervous system causes neurodegeneration in mice. Nature 2006; 441:880-4.
48. Hara T, Nakamura K, Matsui M, Yamamoto A, Nakahara Y, Suzuki-Migishima R, Yokoyama M, Mishima K, Saito I, Okano H, Mizushima N. Suppression of basal autophagy in neural cells causes neurodegenerative disease in mice. Nature 2006; 441:885-9.
49. Coffey ET, Smiciene G, Hongisto V, Cao J, Brecht S, Herdegen T, Courtney MJ. c-Jun N-terminal protein kinase (JNK) 2/3 is specifically activated by stress, mediating c-Jun activation, in the presence of constitutive JNK1 activity in cerebellar neurons. J Neurosci 2002; 22:4335-45.

The print version of this article was created on 19 Sep 2007. This reflects all typographical corrections and errata to the article through that date. Details of any changes may be found in the online version of the article.